Langmuir Article

pubs.acs.org/Langmuir

Comparative Molecular Simulation Study of CO_2/N_2 and CH_4/N_2 Separation in Zeolites and Metal−Organic Frameworks

Bei Liu*,† and Berend Smit†,‡

†Department of Chemical Engineering and ‡Department of Chemistry, University of California, Berkeley, California 94720-1462

Received November 30, 2008

In this work, a systematic molecular simulation study was performed to compare the separation of CO_2/N_2 and CH_4/N_2 mixtures in two different classes of nanoporous materials, zeolites, and metal−organic frameworks (MOFs). For this purpose, three zeolites (MFI, LTA, and DDR) and seven MOFs (Cu-BTC, MIL-47 (V), IRMOF-1, IRMOF-12, IRMOF-14, IRMOF-11, and IRMOF-13) were chosen as the representatives to compare. On the basis of the validated force fields, both adsorption selectivity and pure CO_2 and CH_4 adsorption isotherms were simulated. The results show that although MOFs perform much better for gas storage, their separation performance is comparable to zeolites; for the systems with the preferable component having a larger quadrupolar moment, both zeolites and MOFs can enhance the separation selectivity, and in contrast they both reduce the selectivity. In addition, we show that ideal adsorbed solution theory (IAST) gives a very reasonable prediction of the mixture adsorption isotherms both in zeolites and in MOFs if the pure component isotherms are known. We demonstrate that the difference in quadrupolar moment of the components is an important property that has to be considered in the selection of a membrane material.

1. Introduction

Zeolites are an important class of inorganic microporous materials, which are crystalline silicates or aluminosilicates with three-dimensional (3D) microporous framework structures. In their common form, zeolites are based on TO_4 tetrahedra, where T is an aluminum or silicon atom. The primary building units (PBUs) are the TO_4 tetrahedra, and they form secondary building units (SBUs), such as four rings (4R), five rings (5R), six rings (6R), eight rings (8R), double four rings (D4R), double six rings (D6R), double eight rings (D8R), and so on, that contain up to 16 T atoms. These SBUs assembled together give rise to a large variety of different zeolites.[1] Owing to their structural and compositional features, zeolites have been playing a prominent role in many large-scale applications of gas adsorption and chemical separations for a long time.[2−6]

Recently, a new family of hybrid porous materials that are formed by the coordination of metal ions with organic linkers, namely, metal−organic frameworks (MOFs), appeared and have attracted a great deal of attention as a new addition to microporous materials.[7−11] Similar to zeolites, MOFs can be built up from either tetrahedral or octahedral building blocks and have 3D microporous channels and ultrahigh specific surface areas. Due to the similarity in structure, MOFs are also called "organic" zeolites. However, by varying the linkers, ligands, and metals in the material, their synthesis can readily adapted to control pore connectivity, structure, and dimension, featuring opportunities for a large range of differences in functionality. To date, a large number of different MOFs have been synthesized which have shown various promising applications in, for example, gas storage and separation, and so on.[12−14]

Due to the large number of different zeolites and MOFs that exist, efforts to predict the performance of zeolites and MOFs using molecular modeling can play an important role in selecting materials for specific applications. Although extensive simulation studies have been carried out on the adsorption and separation of gases/gas mixtures in zeolites and MOFs separately,[15−18] far less attention has been given to directly compare the separation performance of these two families of materials. Babarao et al.[19] made a comparison between MFI zeolite and IRMOF-1 for the storage and separation of CO_2 and CH_4. It is known that MFI is only the representative for intersecting channel-type zeolites (commonly, the structures of zeolites are divided in three types, i.e., one-dimensional (1D) channel type, intersecting channels type, and cages separated by windows type[20]), while IRMOF-1 is the simplest and most well-studied MOF with cubic pores. Therefore, a comparison between these two materials cannot give an overall performance of these two families of materials. As

*Corresponding author. E-mail: bei-liu@berkeley.edu.

(1) Baerlocher, C.; McCusker, L. B. *Database of Zeolite Structures*, International Zeolite Association, http://www.iza-structure.org/databases/, 26 June 2001.
(2) Ruthven, D. M. *Principles of Adsorption and Adsorption Processes*; John Wiley: New York, 1984.
(3) Rees, L. V. C.; Shen, D. Adsorption of gases in zeolite molecular sieves. In *Introduction to Zeolite Science and Practice*; van Bekkum, H., Flanigen, E. M., Jacobs, P. A., Jansen, J. C., Eds.; Studies in Surface Science and Catalysis No. 137; Elsevier: Amsterdam, 2001; Chapter 13, pp 579−631.
(4) Kärger, J.; Ruthven, D. M. *Diffusion in zeolites and other microporous solids*; Wiley: New York, 1992.
(5) Auerbach, S. M.; Carrado, K. A.; Dutta, P. K. *Handbook of Zeolite Science and Technology*; Marcel Dekker: New York, 2003.
(6) Smit, B.; Maesen, T. L. M. *Chem. Rev.* **2008**, *108*, 4125.
(7) Moulton, B.; Zaworotko, M. J. *Chem. Rev.* **2001**, *101*, 1629.
(8) Eddaoudi, M.; Moler, D. B.; Li, H.; Chen, B.; Reineke, T. M.; O'Keeffe, M.; Yaghi, O. M. *Acc. Chem. Res.* **2001**, *34*, 319.
(9) Janiak, C. *Dalton Trans.* **2003**, 2781.
(10) Kitagawa, S.; Kitaura, R.; Noro, S.-I. *Angew. Chem., Int. Ed.* **2004**, *43*, 2334.
(11) Ockwig, N. W.; Delgado-Friedrichs, O.; O'Keeffe, M.; Yaghi, O. M. *Acc. Chem. Res.* **2005**, *38*, 176.
(12) Rowsell, J. L. C.; Yaghi, O. M. *Angew. Chem., Int. Ed.* **2005**, *44*, 4670.
(13) Férey, G. *Chem. Soc. Rev.* **2008**, *37*, 191.
(14) Mueller, U.; Schubert, M.; Teich, F.; Puetter, H.; Schierle-Arndt, K.; Pastré, J. *J. Mater. Chem.* **2006**, *16*, 626.
(15) Catlow, C. R. A.; van Santen, R. A.; Smit, B. *Computer Modelling of Microporous Materials*; Elsevier Science: Amsterdam, 2004.
(16) Krishna, R.; Smit, B.; Calero, S. *Chem. Soc. Rev.* **2002**, *31*, 185.
(17) Smit, B.; Maesen, T. L. M. *Nature (London)* **2008**, *451*, 671.
(18) Keskin, S.; Liu, J.; Rankin, R. B.; Johnson, J. K.; Sholl, D. S. *Ind. Eng. Chem. Res.* **2009**, *48*, 2355.
(19) Babarao, R.; Hu, Z.; Jiang, J.; Chempath, S.; Sandler, S. I. *Langmuir* **2007**, *23*, 659.
(20) Beerdsen, E.; Dubbeldam, D.; Smit, B. *Phys. Rev. Lett.* **2006**, *96*, 044501.

zeolites and MOFs are both promising materials for gas storage and separation and they have similarity in structure, it is important to make a systematic study to compare them; such a study not only can get an overall picture on their separation performance but also can provide insights into microscopic level general information that is useful for guiding future microporous materials design and synthesis. To meet this purpose, in this work, we selected three representatives of zeolites (MFI, LTA, and DDR) and seven representatives of MOFs (Cu-BTC, MIL-47 (V), IRMOF-1, IRMOF-12, IRMOF-14, IRMOF-11, and IRMOF-13) as the model adsorbents for separation. The chosen zeolites fall into two categories consisting of intersecting channels (MFI, one of the most important structures in zeolites) and cages separated by windows (LTA and DDR, which have good gas mixture separation abilities[21]). The chosen MOFs represent a typical range of different chemical compositions, pore sizes, and pore topologies. These structures are also representatives of different well-known MOF families in which structures with and without catenation are both included. On the other hand, we selected CO_2/N_2 and CH_4/N_2 systems as the model mixtures to separate, since, first, they are important practical systems that are included in large-scale industrial applications: CO_2/N_2 separation is involved in carbon dioxide capture from flue gas, and separation of N_2 from CH_4 is important in natural gas purification. Second, the characteristics of these two systems are different: CO_2/N_2 contains two components with different quadrupolar moments, while CH_4/N_2 is composed of a nonpolar species CH_4 and a quadrupolar species N_2; this gives more information for understanding the differences in separation performance of zeolites and MOFs. The knowledge obtained is expected to apply to a broad range of zeolites and MOFs for separation of various gas mixture systems of practical importance.

2. Models and Computational Method

2.1. Zeolite and MOF Structures. In this work, the structures of MFI, LTA, and DDR zeolites were constructed using the atomic coordinates reported in the literature.[1] MFI zeolite is perhaps the most well-studied zeolite. It consists of straight 10-ring channels, running in the *y* direction, intersected (in complete intersections) by so-called zigzag channels that run in the *x* and *z* directions, which also consist of 10-membered ring windows. These channels have diameters of approximately 5.4 Å. The structure of LTA zeolite consists of almost spherical cages of about 10 Å in diameter, connected by narrow windows of about 4 Å in diameter. One unit cell consists of 8 cubically arranged cages. DDR zeolite consists of 19-hedron cavities connected through 8R windows across into a hexagonally arranged two-dimensional (2D) cage/window-type system. The structures of these three zeolites can be found in ref 21.

The structures of the selected MOFs were constructed from their corresponding experimental XRD data.[22−24] Among these materials, Cu-BTC is composed of $Cu_2(COO)_4$ paddle wheels with copper dimers as four connectors and benzene-1,3,5-tricarboxylate (BTC) as three connectors, forming a 3D network with main channels of a square cross section of ca. 9 Å diameter and tetrahedral side pockets of ca. 5 Å, which are connected to the main channels by triangular windows of ca. 3.5 Å.[22] MIL-47 (V), which has the chemical formula $M(O)(O_2C-C_6H_4-CO_2)$, where M is vanadium (V^{4+}), possesses corner-sharing oxo groups linking the metal atoms, forming a 3D network with a 1D diamond-shaped tunnel.[23] IRMOFs-1, -12, and -14 feature the same primitive cubic topology with the octahedral $Zn_4O(CO_2)$ clusters linked by different organic dicarboxylate linkers, while IRMOFs-11 and -13 are the catenated counterparts of IRMOFs-12 and -14, respectively.[24] The guest-free crystal structures of these MOFs can be found in previous works.[25−28]

Some details of the structures of the above-mentioned zeolites and MOFs are summarized in Table 1.

2.2. Force Field. To make a reasonable comparison of typical zeolites and MOFs, the force fields employed must be reliable. In this work, the force fields adopted are either taken from literature that have been validated for the systems considered or the parameters are refined by us to give better representation of experimental adsorption data.

Zeolites: CH_4, CO_2, and N_2 Systems. The force field used for zeolites−adsorbates systems in this work is the one used by García-Pérez et al.[29] In this force field, CH_4 molecules were described with a united-atom model, in which each molecule is treated as a single interaction center. CO_2 was modeled as a rigid linear molecule with bond length C−O of 1.16 Å and partial charges distributed around each molecule ($q_O = -0.3256e$ and $q_C = 0.6512e$).[30] The N_2 molecule was represented as a three-site model with two sites located at two N atoms and the third one located at its center of mass (COM). The bond length between two N atoms is 1.098 Å. Each N_2 molecule was assigned a negative charge on each N atom ($q_N = -0.40484e$) and a positive charge at the COM site ($q_{COM} = 0.80968e$).[31] The interactions between adsorbed molecules and zeolite−adsorbates were described with Coulombic and Lennard−Jones (LJ) terms. The LJ parameters for the interaction between adsorbed molecules, the parameters for zeolites−adsorbates interactions, and the static atomic charges of zeolite lattices were all taken from ref 29. This force field has been validated in detail for the adsorption of CH_4, CO_2, and N_2 in several pure silica zeolites.[21,29] For a detailed description of the force field, the reader is referred to ref 29 and Table 1 in the Supporting Information.

MOFs: CH_4, CO_2, and N_2 Systems. For describing the adsorption of pure components and mixtures of CH_4, CO_2, and N_2 molecules in the selected MOFs, methane was modeled as a single-center Lennard−Jones molecule using the TraPPE force field developed by Martin and Siepmann.[32] CO_2 was modeled as a rigid linear molecule with three charged LJ sites located on each atom. A combination of the site−site LJ and Coulombic potentials was used to calculate the CO_2-CO_2 intermolecular interaction. The LJ potential parameters for atoms O and C in CO_2 were taken from the TraPPE force field developed by Potoff and Siepmann.[33] The C−O bond length is 1.16 Å. In this model, partial point charges centered at each LJ site ($q_O = -0.35e$ and

(21) Krishna, R.; van Baten, J. M. *Chem. Eng. J.* **2007**, *133*, 121.
(22) Chui, S. S.-Y.; Lo, S. M.-F.; Charmant, J. P. H.; Orpen, A. G.; Williams, I. D. *Science* **1999**, *283*, 1148.
(23) Barthelet, K.; Marrot, J.; Riou, D.; Ferey, G. *Angew. Chem., Int. Ed.* **2002**, *41*, 281.
(24) Eddaoudi, M.; Kim, J.; Rosi, N.; Vodak, D.; Wachter, J.; O'Keeffe, M.; Yaghi, O. M. *Science* **2002**, *295*, 469.
(25) Yang, Q.; Zhong, C. *ChemPhysChem* **2006**, *7*, 1417.
(26) Ramsahye, N. A.; Maurin, G.; Bourrelly, S.; Llewellyn, P. L.; Devic, T.; Serre, C.; Loiseau, T.; Ferey, G. *Adsorption* **2007**, *13*, 461.
(27) Yang, Q.; Zhong, C. *J. Phys. Chem. B* **2005**, *109*, 11862.
(28) Liu, B.; Yang, Q.; Xue, C.; Zhong, C.; Smit, B. *Phys. Chem. Chem. Phys.* **2008**, *10*, 3244.
(29) García-Pérez, E.; Parra, J. B.; Ania, C. O.; Garcia-Sanchez, A.; van Baten, J. M.; Krishna, R.; Dubbeldam, D.; Calero, S. *Adsorption* **2007**, *13*, 469.
(30) Harris, J. G.; Yung, K. H. *J. Phys. Chem.* **1995**, *99*, 12021.
(31) Murthy, C. S.; Singer, K.; Klein, M. L.; McDonald, I. R. *Mol. Phys.* **1980**, *41*, 1387.
(32) Martin, M. G.; Siepmann, J. I. *J. Phys. Chem. B* **1998**, *102*, 2569.
(33) Potoff, J. J.; Siepmann, J. I. *AIChE J.* **2001**, *47*, 1676.

Table 1. Structural Properties for the Materials Studied in This Work

material	pore shape and size (Å)[a]	unit cell (Å)	cell angle (degree)	ρ_{crys} (g/cm^3)[a]
MFI	intersecting channel, 5.1−5.5/5.3−5.6	a = 20.022, b = 19.899, c = 13.383	$\alpha = \beta = \gamma$ = 90	1.796
LTA	cage/window, 10.0/4.1	$a = b = c$ = 24.555	$\alpha = \beta = \gamma$ = 90	1.294
DDR	cage/window, 8.75/4.5	$a = b$ = 13.860, c = 40.89	$\alpha = \beta$ = 90, γ = 120	1.76
Cu-BTC	pocket/channel, 5.0/9.0	$a = b = c$ = 26.343	$\alpha = \beta = \gamma$ = 90	0.879
MIL-47 (V)	channel, 11.0/10.5	a = 6.818, b = 16.143, c = 13.939	$\alpha = \beta = \gamma$ = 90	1.0004
IRMOF-1	cubic, 10.9/14.3	$a = b = c$ = 25.832	$\alpha = \beta = \gamma$ = 90	0.593
IRMOF-12	cubic, 13.9/20.0	$a = b = c$ = 34.281	$\alpha = \beta = \gamma$ = 90	0.38
IRMOF-14	cubic, 14.7/20.1	$a = b = c$ = 34.381	$\alpha = \beta = \gamma$ = 90	0.373
IRMOF-11	cubic/catenation, 3.5/3.8/4.7/6.1/7.3/11.1	$a = b$ = 24.822, c = 56.734	$\alpha = \beta$ = 90, γ = 120	0.76
IRMOF-13	cubic/catenation, 4.2/4.7/6.1/7.0/11.4	$a = b$ = 24.822, c = 56.734	$\alpha = \beta$ = 90, γ = 120	0.752

[a] Obtained from the XRD crystal data.[1,22−24]

Table 2. Henry Coefficients K_H and Isosteric Heats of Adsorption at Infinite Dilution Q_{st}^0 of CO_2 and CH_4 at 298 K in Cu-BTC

CO_2				CH_4			
K_H (mol/kg/Pa)		Q_{st}^0 (kJ/mol)		K_H (mol/kg/Pa)		Q_{st}^0 (kJ/mol)	
sim.	exp.[a]	sim.	exp.	sim.	exp.[a]	sim.	exp.
5.90×10^{-5}	6.063×10^{-5}	24.958	28.1	1.17×10^{-5}	7.911×10^{-6}	18.394	16.6

[a] The experimental Henry coefficients K_H (mol/kg/Pa) are obtained from $K_H = q_{m,i}K_i^0 \exp(-\Delta H_i/RT)$. Here, $q_{m,i}$ (mol/kg), K_i^0 (bar^{-1}), and $-\Delta H_i$ (kJ/mol) are given in ref 38 and R = 8.31451 J/mol/K.

$q_C = 0.70e$) approximately represent the first-order electrostatic and second-order induction interactions. Again, N_2 was modeled as a diatomic molecule with fixed bond lengths (1.1 Å). In this model, point charges are centered on each LJ site, and electric neutrality is maintained by placing a point charge of $+0.964e$ at the center of mass of the N_2 molecule. The interactions between various sites in the adsorbed molecules were also calculated by the summation of LJ interactions and the electrostatic interactions. The LJ parameters for the N_2 molecule were also taken from the TraPPE force field.[33] For the MOFs studied here, a combination of the site−site LJ and Coulombic potentials were also used to calculate the interactions between adsorbate molecules and adsorbents. In our simulations, all the LJ cross interaction parameters were determined by the Lorentz−Berthelot mixing rules. An atomistic representation was used for all MOFs studied. For calculating the interactions between the adsorbate molecules and the atoms in the framework of the MOF materials, we need to know the atomic partial charges and LJ parameters for the atoms in MOFs.

Cu-BTC. We adopted the atomic partial charges of Cu-BTC from Yang and Zhong.[25] The LJ parameters for Cu-BTC atoms were also taken from ref 25 for CH_4 and CO_2 and from Yang et al.[34] for N_2. These force field parameters were chosen because they have been successfully employed to simulate the adsorption of CH_4, CO_2, and N_2 in Cu-BTC by other researchers.[25,34−37] To further confirm the reliability of the force field adopted, we calculated Henry coefficients K_H and isosteric heats of adsorption at infinite dilution Q_{st}^0 of CO_2 and CH_4 at 298 K in Cu-BTC and compared with experimental data,[38] as shown in Table 2. As can be seen from Table 2, reasonably good agreement between our simulations and the experimental data was obtained.

A detailed description of the force field is given in Table 2 in the Supporting Information.

Table 3. Potential Parameters for the Atoms in the Framework of MIL-47 (V)

	CH_4		CO_2		N_2	
atom	σ (Å)	ε/k_B (K)	σ (Å)	ε/k_B (K)	σ (Å)	ε/k_B (K)
V	2.801[a]	8.056[a]	2.801[a]	8.056[a]	2.801[a]	8.056[a]
O	3.12[a]	26.15[b]	3.12[a]	26.15[b]	3.12[a]	24.15[b]
C	3.43[a]	45.27[b]	3.23[b]	42.27[b]	3.23[b]	40.27[b]
H	2.57[a]	18.14[b]	2.57[a]	18.14[b]	2.57[a]	16.14[b]

[a] Taken from the UFF of Rappé et al.[40] [b] Obtained in this work.

MIL-47 (V). The atomic partial charges for the atoms in MIL-47 (V) were taken from Rosenbach et al.[39] The dispersive interactions of all of the atoms in MIL-47 (V) are described by the universal force field (UFF) of Rappé et al.[40] To better represent the adsorption isotherms of pure CH_4, CO_2, and N_2 in MIL-47 (V), part of the LJ parameters of the UFF were refined in this work, as shown in Table 3. A similar strategy was previously used in our work on zeolites[41−45] and in the work of Yang and Zhong[25,34,35,46] for the adsorption of alkanes, CO_2, N_2, and O_2 in Cu-BTC and several other MOFs.

Our simulation results as well as the experimental data[23,39,47] and previous simulation results[26,39] are shown in Figure 1. We found that except for N_2 the improved parameters yield a significantly better representation of the experimental data.

IRMOFs. The atomic partial charges for the atoms in IRMOFs-1, -12, and -14 were taken from Yang et al.[46] Since the atomic partial charge presented in an atom of a framework is mainly determined by the atoms bonded to it, it is a good approximation to treat the catenated IRMOFs-11 and -13 to

(34) Yang, Q.; Xue, C.; Zhong, C.; Chen, J. *AIChE J.* **2007**, *53*, 2832.
(35) Yang, Q.; Zhong, C. *J. Phys. Chem. B* **2006**, *110*, 17776.
(36) Wang, S.; Yang, Q.; Zhong, C. *Sep. Purif. Technol.* **2008**, *60*, 30.
(37) Karra, J. R.; Walton, K. S. *Langmuir* **2008**, *24*, 8620.
(38) Cavenati, S.; Grande, C. A.; Rodrigues, A. E.; Kiener, C.; Muller, U. *Ind. Eng. Chem. Res.* **2008**, *47*, 6333.
(39) Rosenbach, N.; Jobic, H.; Ghoufi, A.; Salles, F.; Maurin, G.; Bourrelly, S.; Llewellyn, P. L.; Devic, T.; Serre, C.; Férey, G. *Angew. Chem., Int. Ed.* **2008**, *47*, 6611.
(40) Rappé, A. K.; Casewit, C. J.; Colwell, K. S.; Goddard, W. A.III; Skiff, W. M. *J. Am. Chem. Soc.* **1992**, *114*, 10024.
(41) Dubbeldam, D.; Calero, S.; Vlugt, T. J. H.; Krishna, R.; Maesen, T. L. M.; Beerdsen, E.; Smit, B. *Phys. Rev. Lett.* **2004**, *93*, 088302.
(42) Dubbeldam, D.; Calero, S.; Vlugt, T. J. H.; Krishna, R.; Maesen, T. L. M.; Smit, B. *J. Phys. Chem. B* **2004**, *108*, 12301.
(43) Calero, S.; Dubbeldam, D.; Krishna, R.; Smit, B.; Vlugt, T. J. H.; Denayer, J. F. M.; Martens, J. A.; Maesen, T. L. M. *J. Am. Chem. Soc.* **2004**, *126*, 11377.
(44) Calero, S.; Lobato, M. D.; García-Pérez, E.; Mejías, J. A.; Lago, S.; Vlugt, T. J. H.; Maesen, T. L. M.; Smit, B.; Dubbeldam, D. *J. Phys. Chem. B* **2006**, *110*, 5838.
(45) Liu, B.; Smit, B.; Rey, F.; Valencia, S.; Calero, S. *J. Phys. Chem. C* **2008**, *112*, 2492.
(46) Yang, Q.; Zhong, C.; Chen, J. *J. Phys. Chem. C* **2008**, *112*, 1562.
(47) Bourrelly, S.; Llewellyn, P. L.; Serre, C.; Millange, F.; Loiseau, T.; Ferey, G. *J. Am. Chem. Soc.* **2005**, *127*, 13519.

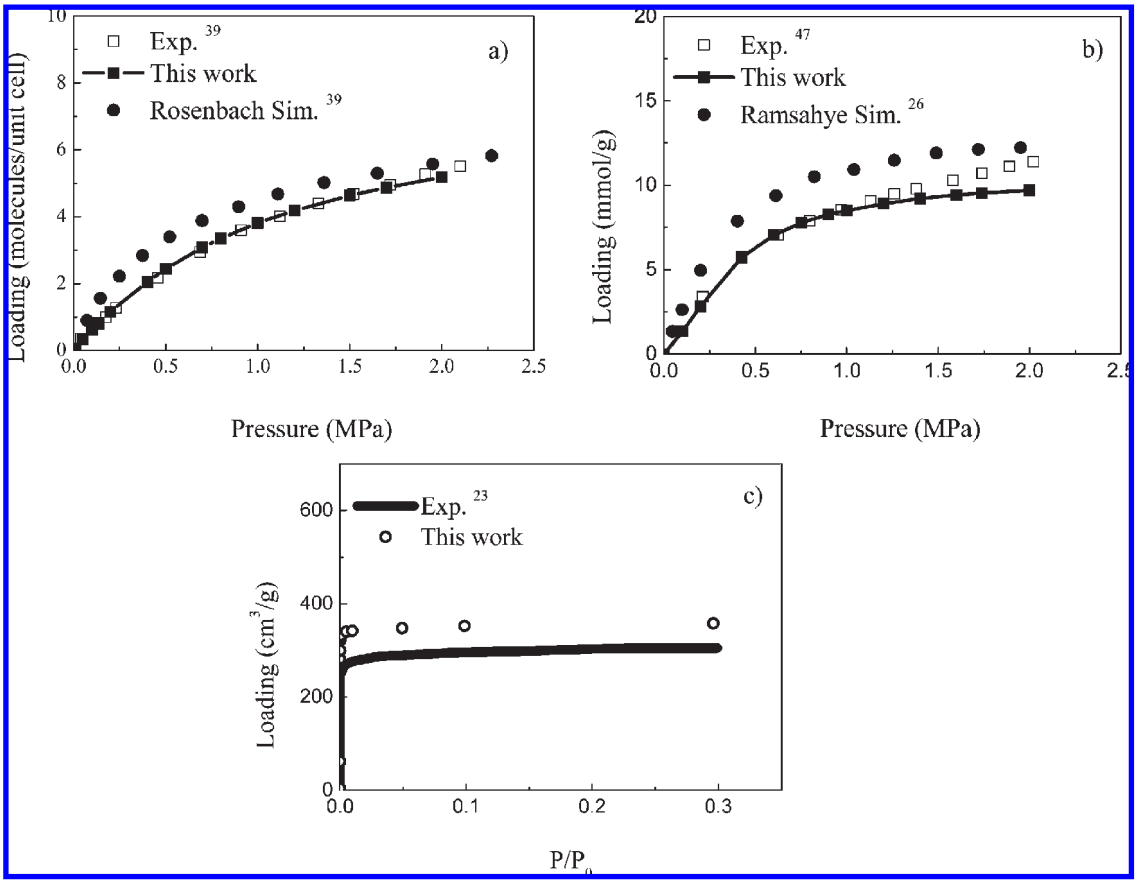

Figure 1. Comparison of the experimental and simulated adsorption isotherms of (a) CH_4 at 303 K, (b) CO_2 at 304 K, and (c) N_2 at 77 K in MIL-47 (V).

have identical atomic partial charges to their corresponding noncatenated counterparts IRMOFs-12 and -14. The LJ parameters for the framework atoms in the IRMOFs were taken from the UFF.[40] This force field has been successfully applied to depict the adsorption of CO_2, CH_4, and their mixtures in MOFs[19,48−52] and shows comparable results with previous simulation[53] using a different force field for N_2 adsorption. A detailed description of the force fields can be found in Tables 3 (IRMOF-1), 4 (IRMOF-11 and IRMOF-12), and 5 (IRMOF-13 and IRMOF-14) of the Supporting Information.

It should be pointed out that though the potential parameter sets used for the adsorbate−adsorbate interactions, that is, CH_4−CH_4, CO_2−CO_2, and N_2−N_2 interactions, are different in zeolites and MOFs. Both sets are equivalently accurate in describing the adsorbate−adsorbate interactions, as all the force fields[30,31,33] can reproduce well the corresponding experimental vapor−liquid coexistence curves and critical properties. The reason why we adopted different adsorbate−adsorbate interaction potential parameters for zeolite and MOF systems is for the consistency of the set of force fields for a given adsorbate−adsorbent system, that is, the consistency between the force fields adopted for adsorbate−adsorbate and adsorbate−adsorbent interactions.

2.3. Simulation Method. Grand-canonical Monte Carlo (GCMC) simulations were employed to calculate the adsorption of pure components and their mixtures in all materials studied. For the calculation of the Henry coefficient and the isosteric heats of adsorption at infinite dilution Q_{st}^0, we performed Monte Carlo simulations in the NVT ensemble. During the simulation, we computed the Rosenbluth factor and the internal energy ΔU, which are directly related to the Henry coefficient and Q_{st}^0, respectively.[42,54] The adsorption simulations were performed at 298 K. The Peng−Robinson equation of state was used to relate the bulk experimental pressure with chemical potential required in the GCMC simulations. Similar to previous works,[6,16−21,25−29,34−37,41−46,49−52,55] all zeolites and MOFs in this work were treated as rigid frameworks, with atoms frozen at their crystallographic positions during the simulations. Several force fields have been developed to take into account the flexibility of zeolites[56−58] and IRMOFs;[59] however, it has been proved that the flexibility of the framework has a negligible influence on the adsorption of gases,[57] although the effect is significant on gas diffusivity.[60] Thus, the treatment of rigid

(48) Garberoglio, G.; Skoulidas, A. I.; Johnson, J. K. *J. Phys. Chem. B* **2005**, *109*, 13094.
(49) Keskin, S.; Sholl, D. S. *J. Phys. Chem. C* **2007**, *111*, 14055.
(50) Babarao, R.; Jiang, J. *Langmuir* **2008**, *24*, 5474.
(51) Babarao, R.; Jiang, J. *Langmuir* **2008**, *24*, 6270.
(52) Liu, B.; Yang, Q.; Xue, C.; Zhong, C.; Chen, B.; Smit, B. *J. Phys. Chem. C* **2008**, *112*, 9854.
(53) Dubbeldam, D.; Frost, H.; Walton, K. S.; Snurr, R. Q. *Fluid Phase Equilib.* **2007**, *261*, 152.
(54) Frenkel, D.; Smit, B. *Understanding Molecular Simulations: From Algorithms to Applications*, 2nd ed.; Academic Press: San Diego, CA, 2002.
(55) Babarao R.; Jiang, J. ; Sandler, S. I. *Langmuir*, published online Dec 18, http://dx.doi.org/.
(56) Demontis, P.; Suffritti, G. B.; Quartieri, S.; Fois, E. S.; Gamba, A. *J. Phys. Chem.* **1988**, *92*, 867.
(57) Vlugt, T. J. H.; Schenk, M. *J. Phys. Chem. B* **2002**, *106*, 12757.
(58) Nicholas, J. B.; Hopfinger, A. J.; Trouw, F. R.; Iton, L. E. *J. Am. Chem. Soc.* **1991**, *113*, 4792.
(59) Dubbeldam, D.; Walton, K. S.; Snurr, R. Q. *Angew. Chem., Int. Ed.* **2007**, *46*, 4496.
(60) Amirjalayer, S.; Tafipolsky, M.; Schmid, R. *Angew. Chem., Int. Ed.* **2007**, *46*, 463.

framework is reasonable. A cutoff radius of 12.0 Å for zeolites and 12.8 Å for MOFs was applied to all the LJ interactions. The long-range electrostatic interactions were handled using the Ewald-summation technique. Periodic boundary conditions were applied in all three dimensions. Since the adsorbent was assumed to be a rigid structure, the potential energies between adsorbate and adsorbent atoms were initially tabulated on a series of three-dimensional grid points with grid spacing 0.15 Å. During the simulations, the potential energy at any position in the adsorbent was determined by interpolation.[48] For each state point, GCMC simulation consisted of 1.5×10^7 steps, to guarantee equilibration, followed by 1.5×10^7 steps to sample the desired thermodynamic properties. The statistical uncertainty was estimated by dividing each run into 10 blocks and calculating the standard deviation from the block averages. The standard deviation is within ±5% for every simulation. A detailed description of the simulation methods can be found in ref 42.

3. Results and Discussion

3.1. Comparison of CO_2/N_2 and CH_4/N_2 Mixture Separation. To give a more comprehensive comparison of the separation performance of zeolites and MOFs, GCMC simulations were performed first for the three zeolites and seven MOFs in separating two binary mixtures, CO_2/N_2 and CH_4/N_2. Ideal adsorbed solution theory (IAST)[61] predictions were then carried out to test if this theory is applicable to the systems considered.

3.1.1. Adsorption Selectivity from GCMC Simulations. In separation processes, a good indication of the ability for separation is the selectivity of a porous material for different components in mixtures. The selectivity for component A relative to component B is defined by $S = (x_A/x_B)(y_B/y_A)$, where x_A and x_B are the mole fractions of components A and B in the adsorbed phase, and y_A and y_B are the mole fractions of components A and B in the bulk phase, respectively. The comparison of the performance of zeolites and MOFs is given in the following paragraphs.

CO_2/N_2 Mixture Separation. Figure 2 shows the adsorption selectivities of CO_2 from the equimolar binary mixture of CO_2/N_2 at 298 K as a function of the bulk pressure up to 2.0 MPa.

In all the adsorbents, CO_2 is more preferentially adsorbed than N_2, and the overall performance of the two families of materials is comparative although the adsorption selectivity does vary among different materials. Among the materials studied, Cu-BTC and MFI show highest selectivity with Cu-BTC performing slightly better. IRMOF-1, IRMOF-12, and IRMOF-14 with large cubic pores give the lowest adsorption selectivity in the pressure range studied. It seems that pore size is an important factor that influences the selectivity for the CO_2/N_2 mixture, and the pore size of ca. 5.0−10.0 Å is the suitable one for this mixture separation. On the other hand, MOFs with catenated structures having various small pores ranging from ca. 3.5 to 11.5 Å (IRMOF-11 and IRMOF-13) also show relatively high selectivity, which is 2−3 times higher than that of their corresponding noncatenated counterparts (IRMOF-12 and IRMOF-14, respectively). This indicates that catenation can enhance the adsorption selectivity for the CO_2/N_2 system. Similar behavior has also been observed in our previous work for the separation of the CH_4/H_2 mixture.[52] An explanation for the reason why pore size is an important influencing factor on selectivity may be that for CO_2/N_2 both of the two components have quadrupolar moment;

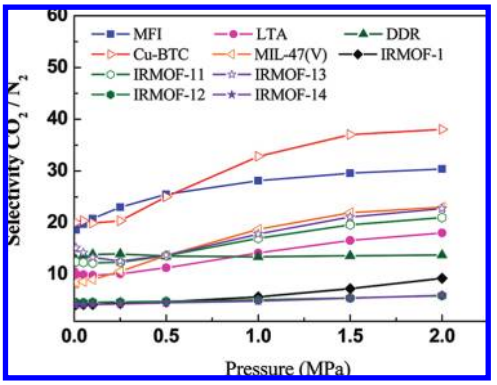

Figure 2. Selectivities for CO_2 as a function of pressure from equimolar binary mixture simulations of CO_2/N_2 at 298 K.

the presence of framework charges and thus electrostatic interactions between adsorbates and adsorbents increases the adsorption of both components in principle, and thus the effect of the chemistry of the materials; that is, the difference of framework atoms which have charges becomes less evident, leading to the result that pore size becomes an important factor. To corroborate this explanation, we carried out additional simulations by switching off all the electrostatic interactions involved by CO_2 and N_2 molecules (case 1) and switching off only the electrostatic interactions of CO_2-adsorbents and N_2-adsorbents (case 2). The calculated adsorption isotherms in (a) MFI zeolite and (b) Cu-BTC, and (c) the corresponding adsorption selectivities of CO_2 from the equimolar binary mixture of CO_2/N_2 in both of them are shown in Figure 3 as a representative, where the results with all of the electrostatic interactions considered are also included (denoted as case 3).

Figure 3a and b shows that when the electrostatic interactions between CO_2, N_2 molecules, and the MFI or Cu-BTC framework are considered (case 3), the amount of CO_2 adsorption increases significantly in both materials compared to cases 1 and 2; however, the amount of N_2 adsorption slightly decreases; this can be attributed to the reason that there is competitive adsorption between CO_2 and N_2 in the materials. Although electrostatic interactions enhance the adsorption of both CO_2 and N_2, they are more beneficial for CO_2 adsorption. Thus, with the increase of the amount of CO_2 adsorption, more adsorption sites are occupied by CO_2 molecules, leading to a slight decrease in N_2 adsorption. This results in a much higher selectivity for the CO_2/N_2 mixture in both materials when the electrostatic interactions between adsorbates and adsorbents are considered, as shown in Figure 3c. Simulations in other zeolites and MOFs were also performed showing similar behavior (see Figure 1 in the Supporting Information). These results suggested that the electrostatic field in the materials, whether zeolites or MOFs, influences the CO_2/N_2 mixture separation in a similar way, and thus, the effect of the chemistry of the materials, that is, the difference of framework atoms which have charges, becomes less evident, leading to the result that pore size becomes an important factor.

CH_4/N_2 Mixture Separation. The second system considered in this work is CH_4/N_2 mixture separation. The adsorption selectivities of CH_4 from the equimolar binary mixture of CH_4/N_2 are shown in Figure 4. Interestingly, the performances of the zeolites and MOFs are different from those for the CO_2/N_2 system as shown in Figure 2: all of the chosen zeolites show better performance than the MOFs adopted in this case; the only similarity is that again IRMOF-1, IRMOF-12, and IRMOF-14 with simple large cubic pores show lowest adsorption selectivity.

(61) Myers, A. L.; Prausnitz, J. M. *AIChE J.* **1965**, *11*, 121.

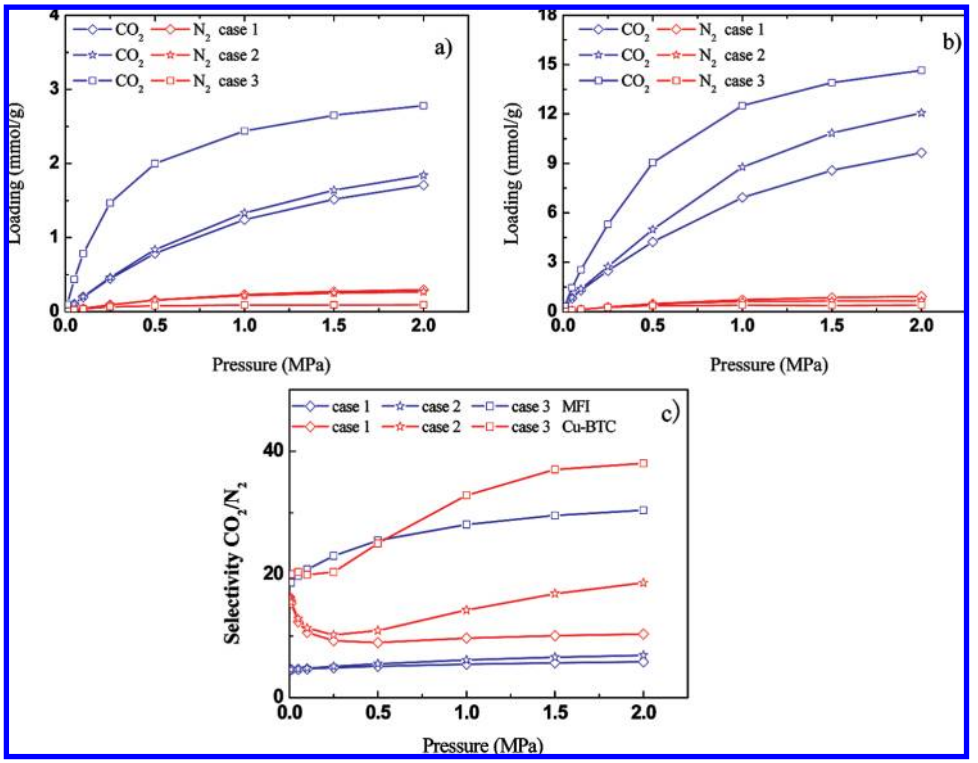

Figure 3. Effect of the electrostatic interactions on the adsorption isotherms of CO_2/N_2 mixture in (a) MFI and (b) Cu-BTC, and (c) the adsorption selectivities for CO_2 from equimolar binary mixture of CO_2/N_2 in MFI and Cu-BTC.

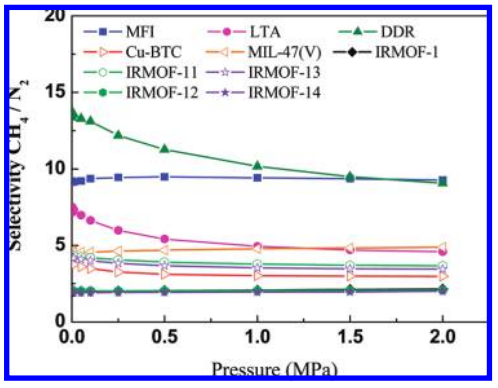

Figure 4. Selectivities for CH_4 as a function of pressure from equimolar binary mixture simulations of CH_4/N_2 at 298 K.

The CH_4/N_2 system contains two components that are much different in chemistry: CH_4 is a difficultly polarized substance, while N_2 is an easily polarized one with weak quadrupolar moment. Similar to CO_2/N_2, we carried out additional simulations to investigate the effect of the electrostatic interactions on the separation of the CH_4/N_2 mixture, and the results of MFI and Cu-BTC are given in Figure 5 as an example. Simulations in other zeolites and MOFs were also performed, and the results are given in Figure 2 in the Supporting Information. Again, in case 1, all the electrostatic interactions involved by N_2 molecules are switched off, in case 2 only the electrostatic interactions between the N_2 molecules and the zeolite or MOF framework are switched off, and in case 3 all the electrostatic interactions are included. Figure 5 shows that the electrostatic field in zeolites and MOFs can enhance the adsorption of gases with quadrupolar moment, that is, N_2 in this case, resulting in negative contribution to the selectivity of CH_4 from the CH_4/N_2 system. Different from CO_2/N_2 mixture separation, it seems that the electrostatic field in zeolites has a stronger effect on N_2 adsorption than in MOFs, resulting in a bigger negative contribution to the selectivity of CH_4 from the CH_4/N_2 system (see Figure 5c). Therefore, not only the pore size and pore topology but also the chemical characteristics of the materials also influence the separation efficiency of the system considered.

The two mixtures CO_2/N_2 and CH_4/N_2 provide a representative example to reveal the relationship between material structure and separation performance. From the comparative study of zeolites and MOFs, it seems that, for a mixture with components similar in quadrupolar moment, pore size plays an important role in determining separation capability. While for those with components largely different in quadrupolar moment, the chemical characteristics of the material also play an important role.

It should be pointed out that, in this work, instead of finding the optimal pressure for the chosen model separation systems, we focus on making a comparison of the separation performances of zeolites and MOFs. From a practical application point of view, CO_2/N_2 separation is involved in CO_2 capture from flue gases and this process is carried out around 0.1 MPa. While for the separation of CH_4 from N_2, it is involved in natural gas purification, which can be operated up to moderate pressure. Therefore, the results obtained in a wide pressure range can be used for future reference for comparing the separation abilities of zeolites and MOFs.

Furthermore, the ratio of CO_2 selectivity from CO_2/N_2 to CH_4 selectivity from CH_4/N_2 was calculated, as given in Figure 6.

Figure 6 shows that, generally speaking, the studied MOFs perform better than zeolites. The reason why Cu-BTC performs much better can be attributed to the fact that it has exposed metal sites, which haven been found to have a strong effect on the separation of polar/nonpolar mixtures[37] and mixtures with different quadrupolar moments.[25,34,55] The existence of exposed metal sites increases the amount of adsorption for those species with larger quadrupolar moment, especially at low loadings. To clarify this, we analyzed the differences of isosteric heats of

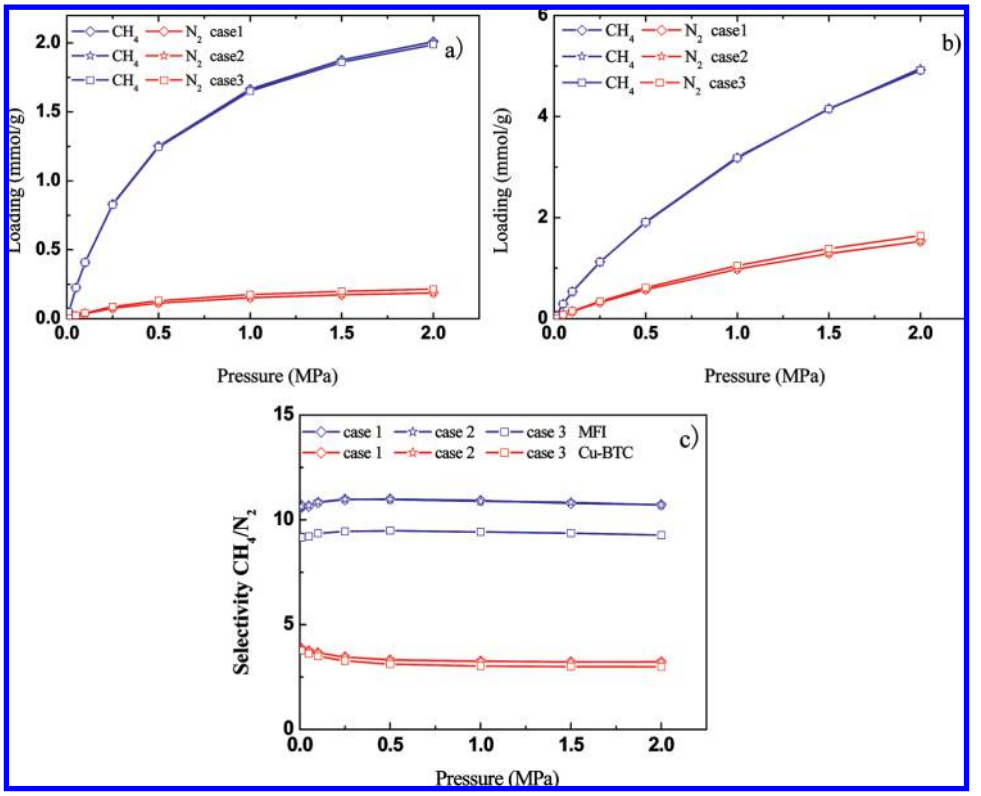

Figure 5. Effect of the electrostatic interactions on the adsorption isotherms of CH_4/N_2 mixture in (a) MFI and (b) Cu-BTC, and c) the adsorption selectivities for CH_4 from equimolar binary mixture of CH_4/N_2 in MFI and Cu-BTC.

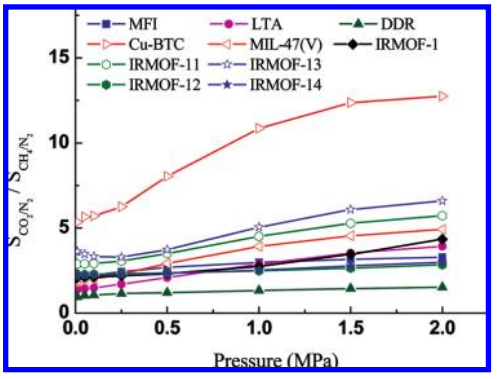

Figure 6. Comparison of selectivities for CO_2 as a function of pressure from equimolar binary mixtures simulations of CO_2/N_2 and CH_4 from equimolar binary mixtures of CH_4/N_2 at 298 K.

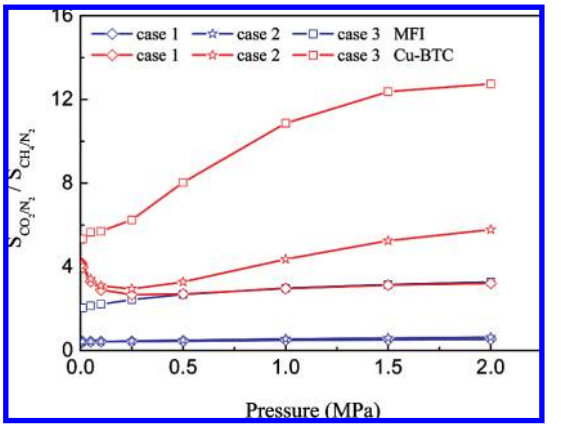

Figure 7. Effect of electrostatic interactions on adsorption selectivities for CO_2 from equimolar binary mixture simulations of CO_2/CH_4 in Cu-BTC and MFI.

adsorption at infinite dilution Q_{st}^0 of CO_2 and CH_4 in Cu-BTC and one type of zeolite, say MFI. The difference of $Q_{stCO_2}^0$ and $Q_{stCH_4}^0$ in Cu-BTC is 6.564 kJ/mol, which is bigger than that in MFI zeolite (4.27 kJ/mol); this explains the larger selectivity observed in Cu-BTC at low loadings. Generally speaking, at intermediate and high loadings, not only the enthalpy effect but also the entropy effect on adsorption is important as well. The adsorption selectivity behavior in this region is the result of the cooperative effects of many factors, such as the chemistry of materials (the different framework atoms which have charges), pore size, and pore topology. To figure out which factor is more important for the separation of the CO_2/CH_4 mixture, we further carried out simulations to investigate the effect of the electrostatic interactions on the separation of the CO_2/CH_4 mixture in Cu-BTC and MFI, and the results are given in Figure 7. Cases 1, 2, and 3 are same as the ones in Figures 3c and 5c.

Evidently, the selectivity of CO_2 from the CO_2/CH_4 mixture can be enhanced in Cu-BTC and MFI with the presence of the framework charges, and due to the preferable component CO_2 has a much larger quadrupolar moment than CH_4. Compared to MFI, Cu-BTC exhibits a larger effect of framework charges on CO_2/CH_4 separation. It seems the chemistry of materials (the different framework atoms which have charges) plays a more important role at intermediate and high loadings for CO_2/CH_4 separation.

3.1.2. IAST Predictions. It has been commonly recognized that ideal adsorbed solution theory (IAST)[61] can give good predictions of gas mixture adsorption in many zeolites[62,63] as

(62) Goj, A; Sholl, D. S.; Akten, E. D.; Kohen, D. *J. Phys. Chem. B* **2002**, *106*, 8367.
(63) Challa, S. R.; Sholl, D. S.; Johnson, J. K. *J. Chem. Phys.* **2002**, *116*, 814.

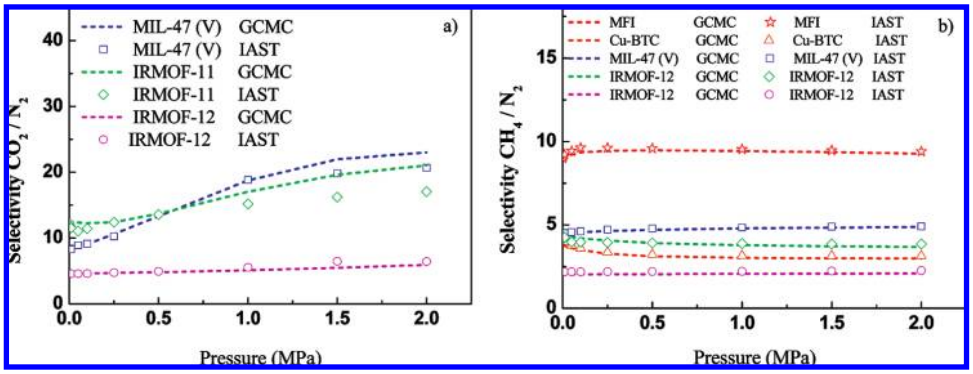

Figure 8. Comparison of IAST and GCMC for (a) CO_2 selectivity as a function of pressure from equimolar binary mixture of CO_2/N_2 and (b) CH_4 selectivity from equimolar binary mixture of CH_4/N_2 at 298 K.

Table 4. Henry Coefficients K_H (mol/kg/Pa) and Isosteric Heats of Adsorption at Infinite Dilution Q_{st}^0 (kJ/mol) of CO_2 and CH_4 in Zeolites and MOFs at 298 K as Obtained from the Simulations

	CO_2		CH_4	
material	K_H	Q_{st}^0	K_H	Q_{st}^0
MFI	1.96×10^{-5}	24.397	9.74×10^{-6}	20.127
LTA	1.04×10^{-5}	22.340	7.79×10^{-6}	19.196
DDR	2.15×10^{-5}	25.410	2.48×10^{-5}	26.369
Cu-BTC	5.90×10^{-5}	24.958	1.17×10^{-5}	18.394
MIL-47(V)	1.45×10^{-5}	19.548	8.11×10^{-6}	14.677
IRMOF-1	8.46×10^{-6}	14.372	4.01×10^{-6}	9.983
IRMOF-11	5.39×10^{-5}	24.433	2.00×10^{-5}	19.644
IRMOF-13	5.90×10^{-5}	24.224	1.91×10^{-5}	18.780
IRMOF-12	1.41×10^{-5}	15.672	6.13×10^{-6}	10.334
IRMOF-14	1.29×10^{-5}	14.750	5.85×10^{-6}	9.850

well as in MOFs.[19,34,35,52,64] If IAST is found to be accurate for a particular class of adsorbates and adsorbents, then further detailed calculations of mixture equilibria are unnecessary to assess adsorption selectivity. It has been demonstrated that it is applicable for depicting CO_2/N_2 adsorption in MFI,[62] LTA, DDR,[65] and Cu-BTC[34] and for depicting CH_4/N_2 in LTA and DDR.[65] IAST calculations were further performed in this work to check whether it is applicable for other cases that have not been tested before. The calculated adsorption selectivities of CO_2 from equimolar mixture CO_2/N_2 in MIL-47(V), IRMOF-11, and IRMOF-12 and those of CH_4 from equimolar mixture CH_4/N_2 in MFI, Cu-BTC, MIL-47(V), IRMOF-11, and IRMOF-12 with GCMC and IAST are shown in Figure 8 as examples. In all the cases, good agreement between GCMC simulation and IAST calculation was obtained, indicating that IAST is applicable to predict the adsorption behavior of CO_2/N_2 and CH_4/N_2 mixtures in most zeolites and MOFs.

3.2. Adsorption of Pure CO_2 and CH_4. In addition to separation applications, both zeolites and MOFs have potential applications in gas storage. Therefore, we further investigated the adsorption properties of pure CO_2 and CH_4 in these materials to make a comprehensive comparison. In the meantime, such research can contribute to guide the development of new nanoporous materials for CO_2 capture and natural gas storage.[46,51,66,67] In this work, Henry coefficients and isosteric heats of adsorption at infinite dilution, and the adsorption isotherms of CO_2 and CH_4 in the 10 materials as a function of pressure up to 6 MPa were calculated, as shown in Table 4 and Figure 9, respectively. The figures up to 6 MPa may not be practical for some applications; however, the results obtained can be used for future reference from both scientific and practical points of view for comparing the adsorption capacities between MOFs and zeolites.

Table 4 and Figure 9 show that, for both CO_2 and CH_4, the three zeolites and the MOFs with small pores (Cu-BTC, IRMOF-11, and IRMOF-13) give comparable isosteric heats of adsorption at infinite dilution Q_{st}^0, which are much larger than those of the other MOFs with large pores. As a result, the three zeolites and the MOFs with small pores give larger adsorption at low pressures. However, at higher pressures, all the MOFs studied in this work can store more CO_2 and CH_4 than the chosen zeolites. Particularly, the MOFs with low framework density and high free volume, such as IRMOF-12 and IRMOF-14, perform best. This demonstrates that MOFs are more promising materials for the storage of CO_2 and CH_4. The adsorption capacity of a material is affected by various factors, and the main ones are accessible surface area (S_{acc}), the interactions between adsorbate and adsorbent (usually it can be characterized by the isosteric heat of adsorption at infinite dilution Q_{st}^0), packing of adsorbate molecules inside the void spaces of the adsorbent, adsorbent framework density (ρ_{crys}), and the available void volumes (V_{free}). Generally speaking, besides a strong affinity with adsorbate molecules, a high quality adsorbent should also possess large accessible surface area, ideal pore topology, low adsorbent framework density, as well as high free volume. Evidently, the adsorption behavior shown in Figure 9 is the result of the cooperative effects of these main influencing factors.

In addition, the different adsorption behaviors of these materials can be rationalized by considering the relative range of the dispersive and electrostatic potentials created by the zeolite and MOF frameworks. We found for the materials with the same chemical composition and similar densities, such as MFI and DDR, IRMOF-12 and IRMOF-14, and IRMOF-11 and IRMOF-13, the amount of adsorbed CH_4 is almost same for each of the pairs and even the pore structures of each pair of materials are different. This can be attributed to the reason that the strength of the dispersive potential is mainly determined by the spacing and density of O atoms in the zeolite framework and of all atoms in the MOF framework near an adsorbed molecule, so this potential is not strongly affected by the large-scale structure of the crystalline material in a series of materials with the same chemical composition and similar densities.[62] The electrostatic potential, in contrast, is a long-range potential and is therefore more sensitive to the large-scale structure of the crystalline adsorbent. Therefore, the adsorbed CO_2 is somehow different in these pairs of materials.

(64) Keskin, S.; Liu, J.; Johnson, J. K.; Sholl, D. S. *Langmuir* **2008**, *24*, 8254.
(65) Krishna, R.; van Baten, J. M. *Sep. Purif. Technol.* **2008**, *61*, 414.
(66) Düren, T.; Sarkisov, L.; Yaghi, O. M.; Snurr, R. Q. *Langmuir* **2004**, *20*, 2683.
(67) Wang, S. *Energy Fuels* **2007**, *21*, 953.

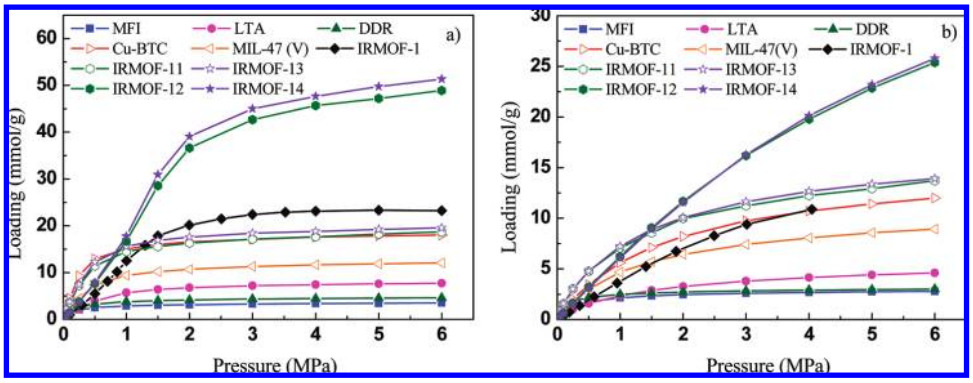

Figure 9. Simulated absolute adsorption isotherms of (a) CO_2 and (b) CH_4 in zeolites and MOFs as a function of pressure.

4. Conclusions

The comparative study of this work on three zeolites and seven MOFs for the storage of CO_2 and CH_4, and the separation of CO_2/N_2 and CH_4/N_2 show that the separation performance is comparable that depends on the nature of the systems to separate. For the systems where the preferable component has a larger quadrupolar moment, both zeolites and MOFs can enhance the separation selectivity. On the contrary, if the preferable component has a smaller quadrupolar moment, they both reduce the selectivity. We performed additional IAST predictions, which show that IAST gives a very reasonable prediction of the mixture adsorption isotherms on the basis of the pure component data for most zeolites and MOFs. We have shown that a good storage material does not guarantee that it is also a good separation material. The difference in quadrupolar moment of the components is an important property that has to be considered in the selection of a membrane material.

Supporting Information Available: The force field parameters for adsorbate−adsorbate, adsorbate−zeolites, and adsorbate-MOFs, the effect of electrostatic interactions on the adsorption isotherms of CO_2/N_2 and CH_4/N_2 mixtures, the effect of electrostatic interactions on the adsorption selectivities for CO_2 from equimolar binary mixture simulations of CO_2/N_2, and the effect of electrostatic interactions on the adsorption selectivities for CH_4 from equimolar binary mixture simulations of CH_4/N_2 in LTA, DDR, MIL-47 (V), IRMOF-1, IRMOF-11, IRMOF-12, IRMOF-13, and IRMOF-14. This material is available free of charge via the Internet at http://pubs.acs.org.